INTEGRATED TESTING OF ELECTRIC VEHICLE THERMAL MANAGEMENT AND OPTIMIZATION OF FLOW FIELD UNIFORMITY IN AIR SUPPLY SYSTEM

YU FU [12], Haitao MIN[1], Weiyi SUN[1 *], Yang Fang [3]

[*1]State Key Laboratory of Automotive Simulation and Control, ChangChun,china 130022

[2]CATARC New Energy Vehicle Test Center (TianJin) Co.,Ltd., TianJin,china 300300

[3]General Research and Development Institute, China FAW Corporation Limited, Changchun,china 130013

[*] Corresponding author; E-mail: swy_18@jlu.edu.cn

Abstract：To meet the requirements of integrated testing and performance calibration for the early development of electric vehicle thermal management, this paper conducted research on the configuration scheme design of the electric vehicle thermal management integrated testing platform and simulation and optimization of the air supply system flow field. Firstly, a requirement analysis of the testing environment and the overall design of the testing platform was performed. Secondly, simulation techniques were applied to optimize the uniformity of the intake airflow field in the test section, which was then validated through real testing. Finally, a comparative study of the tested system was conducted through CFD simulations in two different environments, the testing platform and the actual vehicle underhood.The results indicate that the intake airflow field uniformity in the test section falls within ±3%. The intake flow rate errors for the radiator and condenser, compared to those in the actual vehicle, were found to be 0.039% and 2.116%, respectively. These findings confirm that the testing platform offers good consistency with the flow field in real vehicle testing scenarios.

Keywords: Thermal management; bench test; integrated design; air supply system;Flow field simulation

1 PREFACE

To enhance the safety and comfort of electric vehicles while reducing energy consumption, the design of the electric vehicle thermal management system is trending towards integration, with a highly unified system structure, strong inter-subsystem energy coupling, and intricate control strategies[1]. The strong coupling of energy between the power electronics, electric drive, and thermal management systems increases the complexity of development. In the development process, extensive integrated thermal management performance testing at the system level is required as a prerequisite for testing. Considering the strong coupling between various systems in pure electric vehicles, the integrated testing should encompass the core systems of power electronics, electric drive, thermal management, and control. These system components should be integrated into a test rig, replicating the actual operating environment of the vehicle's components, thus creating an "equivalent to a small real vehicle." This allows for the comprehensive testing of system performance at the system level, guiding

Corresponding Author: Sun Weiyi, Lecturer, Ph.D., E-mail: swy_18@jlu.edu.cn.

development optimization. Lv Feng developed a vehicle-mounted thermal management integrated testing system based on physical components in commercial vehicle cabins. This system can monitor variables like flow rates, temperatures, pressures, vehicle speed, engine speed, and throttle position, establishing relationships between these elements[2]. However, it focuses on testing actual vehicles, and the testing phase still lags behind. Zhao Yibo conducted an in-depth study on the thermodynamic model of a thermal management system test bench, enabling the calculation of parameters like dry bulb temperature, wet bulb temperature, pressure, air flow rate, cooling capacity, and heating capacity[3]. However, this test bench only exists as a model and lacks physical testing hardware for specific experiments. Han Song built a comprehensive test rig consisting of an engine test rig, an in-vehicle testing system, and a wind tunnel system. However, it only tests the engine cooling circuit and doesn't cover other systems, preventing it from conducting multi-system integrated tests. Wang Weimin and others modified a heat pump test bench to verify the performance of the heat pump system in pure electric vehicles[4]. They added some water circuits to the test bench to test the heat pump system's performance and calibrate optimal control parameters such as compressor speed, expansion valve opening, and subcooling. However, this test bench only focuses on the heat pump system's performance and does not include the electric drive system and battery system's thermal management circuits, making it unable to test multi-system coupling performance. Xue Song and others developed a multi-system integrated test rig based on real components of electric vehicles, including the power electronics, electric drive, thermal management, and control core systems[5]. However, this test rig does not control the flow field and temperature field, allowing only for functional and room temperature performance testing and preventing it from conducting high and low-temperature performance testing. Jing Ma placed the tested system in an environmental chamber where the relative positions of the components could be maintained[6]. The environmental chamber provides environmental boundary conditions such as temperature, humidity, and flow field for the tested components. However, the differences in temperature, humidity, and flow field environments in which the electric drive system, battery system, and air conditioning system operate in real vehicle operation are significant. Therefore, the environmental chamber can only provide a single environment and cannot simulate the working environment consistent with the actual vehicle for the tested components. In summary, the existing research breaks the relative positions and coupling relationships between components, with test equipment providing only a single test environment for the tested system without controlling the flow field and temperature field in different component areas. In actual driving, the environmental conditions in different areas inside the vehicle vary significantly. Therefore, there is an urgent need to develop an electric vehicle thermal management integrated test system that can carry the core components of the vehicle, maintain the real relative positions of the components, and simulate the environments in which the components operate. This is to meet the initial development requirements of electric vehicles for integrated thermal management performance testing and performance calibration, to validate system performance early, reduce development risks, and significantly shorten the development time. In response to the shortcomings of existing research and the design principles of testing environment scenario and testing condition operationalization, this paper first starts with an analysis of the working principles of the tested system and the environmental requirements for key components' testing. It proposes and designs the overall configuration and operating principles of the electric vehicle thermal management integrated test platform, completing the construction of the testing environment scenario. A particular focus is placed on the simulation

Corresponding Author: Sun Weiyi, Lecturer, Ph.D., E-mail: swy_18@jlu.edu.cn.

analysis and optimized design of the airflow system in the test platform, and the optimization and empirical verification of the uniformity of the inflow airflow field at the entrance to the test section. This provides a foundational assurance for precise control of the inflow air volume. Finally, to verify the consistency of the flow field environment provided by the test platform and the actual vehicle environment, a comparative CFD simulation study is conducted on the tested system based on both the test platform and the actual vehicle underhood environment.

2 Design Requirements Analysis

The environmental conditions in different areas of vehicles vary greatly,with differences in the underhood environment, air conditioning core environment, and battery environment[7~9].The following will provide a detailed analysis of the demand environment for core components in the three major spaces.

2.1 Analysis of Environmental Requirements for underhood Internal Components

The electric drive system and front-end cooling module are the core components in the cabin. The process of converting electrical energy into mechanical energy in the electric drive system will generate energy loss, mainly including iron core loss, winding loss, and mechanical loss.The internal cooling cycle of the motor carries away a portion of the heat, and its calculation formula is as follows,as the Eq. 1~3:

$$P_w = \rho_w C_w A_w v(T_{in} - T_{out}) \tag{1}$$

ρ_w is the density of the coolant; C_w is the specific heat capacity of the coolant; A_w is the cross-sectional area of the cooling pipeline; v is the flow rate of the coolant;; T_{in} 、 T_{out} are respectively refer to the inlet and outlet temperatures.

The dissipation power loss of the stator and its winding to the surrounding environment:

$$P_{s\_air} = \frac{\delta A_s (T_S - T_0)}{t_2 - t_1} \tag{2}$$

δ is the convective heat transfer coefficient; A_s is the convective heat transfer area on the surface of the stator and winding; T_S is the surface temperature of the stator and winding; T_0 is the ambient temperature; t_2 、 t_1 are the starting and ending time points within a unit time.

The convective heat transfer coefficient is calculated using the following empirical formula:

$$\delta = 9.73 + 14V^{0.62} \tag{3}$$

V is the airflow velocity of the heat dissipation surface.

In summary, it can be seen that the heat generation of the motor is directly related to the operating conditions. The dissipated power of the stator and its winding to the surrounding environment is affected by the environmental temperature and convective heat transfer coefficient, while the convective heat transfer system is also related to the air flow velocity on the heat dissipation surface. Therefore, an integrated thermal management testing system needs to provide operating load conditions, temperature and flow field conditions similar to those in the engine compartment during actual vehicle operation for the electric drive system. To ensure that the flow field distribution around the electric drive system is consistent with the actual vehicle, and to ensure accurate air intake, the

Corresponding Author: Sun Weiyi, Lecturer, Ph.D., E-mail: swy_18@jlu.edu.cn.

airflow velocity distribution at the entrance of the test section should be consistent with the airflow velocity distribution entering the engine room, as uniform as possible.

2.2 Analysis of environmental requirements inside the air conditioning box

The core components inside the air conditioning box are evaporators, built-in condensers, or heater cores. Taking the heater core as an example, the heat transfer calculation formula is as follows[10],as the Eq. 4~8:

$$\Phi = KA\,\Delta t_m \tag{4}$$

$$K = (\beta/h_1 + (\beta * \lambda_3) + (1/\eta_0 * h_2) + R_f)^{-1} \tag{5}$$

$$h = \mu_u * k/L \tag{6}$$

$$\mu_u = C * R_e \tag{7}$$

$$Re = u * d/v \tag{8}$$

Φ is the heat transfer coefficient, K is the heat transfer coefficient, A is the heat transfer area, Δt_m is the logarithmic average temperature difference between the cold and hot fluids, β Is the rib coefficient, h_1 is the surface heat transfer coefficient on the water side, h_2 is the surface heat transfer coefficient on the air side, λ_3 is the thermal conductivity coefficient of the pipe material, R_f is the total thermal resistance between the water side and the air side, h is the surface heat transfer coefficient, L is the characteristic scale of the heat exchange surface, Re is the Reynolds number, d is the pipe diameter, and u is the average flow velocity in the pipe, ν It is a viscous system of liquid motion. From the principle of core heat transfer, it can be seen that the heat transfer performance is directly related to the ambient air temperature and the flow rate through the core.The heat transfer coefficient of the evaporator and built-in condenser is also related to the temperature and flow rate of the gas passing through its core surface. Therefore, an integrated thermal management testing system needs to provide target temperature and precise air supply for the components inside the air conditioning box.

2.3 Analysis of environmental requirements around the power battery system

Taking lithium iron phosphate battery as an example, the mathematical control equation for its three-dimensional electrically thermally coupled mode is [11],as the Eq. 10~18:

$$\rho_p C_p \frac{\partial T}{\partial \tau} = k_{px}\frac{\partial^2 T}{\partial x^2} + k_{py}\frac{\partial^2 T}{\partial y^2} + k_{pz}\frac{\partial^2 T}{\partial z^2} + \dot{q}_p - \dot{q}_{fp} \tag{9}$$

$$\rho_n C_n \frac{\partial T}{\partial \tau} = k_{nx}\frac{\partial^2 T}{\partial x^2} + k_{ny}\frac{\partial^2 T}{\partial y^2} + k_{nz}\frac{\partial^2 T}{\partial z^2} + \dot{q}_p - \dot{q}_{fn} \tag{10}$$

$$\rho_r C_r \frac{\partial T}{\partial \tau} = k_{rx}\frac{\partial^2 T}{\partial x^2} + k_{ry}\frac{\partial^2 T}{\partial y^2} + k_{rz}\frac{\partial^2 T}{\partial z^2} + \dot{q}_p - \dot{q}_{fr} \tag{11}$$

$$\dot{q}_p = J_p(U_0 - U - T\frac{dU_0}{dT}) + I_p^2 R_{pp} \tag{12}$$

$$\dot{q}_n = J_n(U_0 - U - T\frac{dU_0}{dT}) + I_n^2 R_{pn} \tag{13}$$

$$\dot{q}_r = 0 \tag{14}$$

$$J_p = \sigma_{cp}.\Delta\phi p \tag{15}$$

$$J_n = \sigma_{cn}.\Delta\phi n \tag{16}$$

$$\Delta\phi_p = \frac{I_{tp}}{\sigma_{cp}^h p^s p} \tag{17}$$

Corresponding Author: Sun Weiyi, Lecturer, Ph.D., E-mail: swy_18@jlu.edu.cn.

$$\Delta\phi_n = \frac{I_{tp}}{\sigma_{cn}^{h} n^{s} n} \tag{18}$$

$\dot{q}_p$ $\dot{q}_n$ $\dot{q}_r$ are the heat production rates of the positive electrode current collector, the negative electrode current collector, and the battery plate, respectively, $W \cdot m^{-3}$; R_{pp} R_{pn} are equivalent polarization internal resistance of the positive and negative plate current collectors,Ω; σ_{cp} σ_{cn} are the conductivity of the positive and negative electrode plates, $S \cdot m^{-1}$; $\Delta\phi_p$ $\Delta\phi_n$ are potential differences within the positive and negative electrode plates are respectively,V; I_{tp} I_{tn} are the currents flowing through the positive and negative electrode plates.

From the heat generation model of the power battery system, it can be seen that the heat generation of the battery is influenced by operating conditions and internal resistance. The size of the internal resistance of the battery is related to temperature[12]. Research has shown that when the battery temperature decreases by 5 ℃, the internal resistance increases by 35m Ω[13]. The lower the ambient temperature of the battery, the greater its internal resistance value, and the higher its heat generation[12]. Therefore, the heat generation of the battery is related to the ambient temperature. The heat transfer methods of batteries can be divided into three types,thermal conduction, thermal convection, and thermal radiation. Currently, the mainstream cooling methods for batteries in the industry are liquid cooling and direct cooling. The bottom of the battery is separated from the battery surface by a partition, and the convective heat transfer between the battery surface and the external airflow can be ignored. However, the high temperature of the asphalt ground in summer cannot ignore its thermal radiation to the battery. In summary, the integrated thermal management testing system needs to provide the power battery system with temperature environment, ground radiation, and real operating load similar to that of the battery under actual vehicle operation.

Based on the above analysis, it can be concluded that the testing system needs to provide real operating loads for the electric drive system, target temperature, humidity, and precise and uniform air supply for the internal components of the cabin. Provide target temperature, humidity, and precise air supply for the heat exchanger in the air conditioning box, and provide temperature and ground radiation environment for the power battery system. Based on the analysis of the environmental conditions required for each region, the platform needs to be equipped with a temperature control system, humidity control system, and air supply control system. Each system is independently controlled to provide target environments for each region. The platform requirements and system configuration are shown in Figure 1.

Corresponding Author: Sun Weiyi, Lecturer, Ph.D., E-mail: swy_18@jlu.edu.cn.

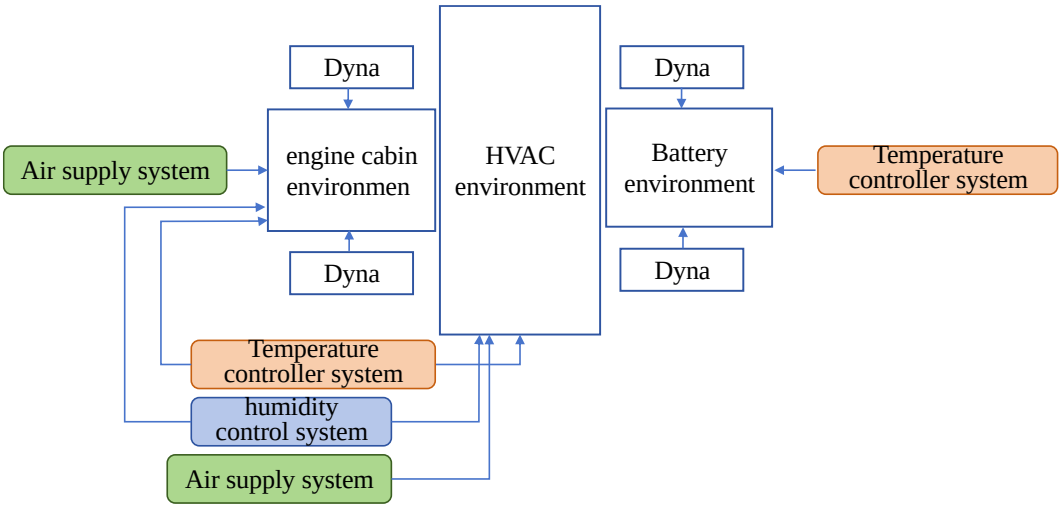

Fig. 1 Test environment requirements and system configuration for each system

3 Research on the overall design of the system

3.1 Overall System Configuration and Operating Principles

According to the above analysis conclusion, the system scheme includes simulated underhood environment air duct that is independent of each other, simulated HVAC (heating ventilation and air conditioning) environment air duct, simulated battery temperature control box, and two sets of dynamometers. The layout fully considers the true position of electric vehicle components, pipeline length, and compact structure. The specific structural form is shown in Figure

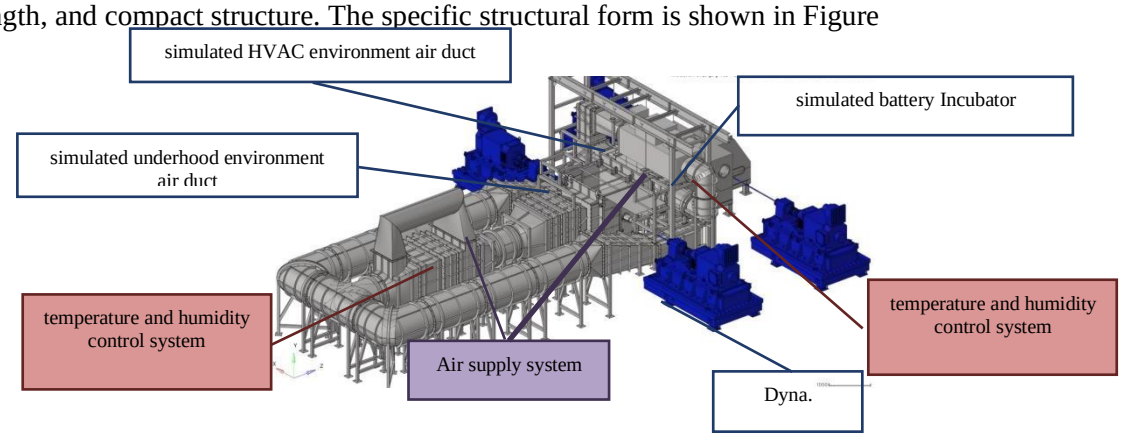

Fig. 2 Schematic diagram of system layout structure

The environmental conditions in the system are achieved by the air supply system,the temperature control system and humidity control system, and the operating principle diagram is shown in Figure 3. The temperature control of the simulated underhood environment air duct and the simulated HVAC environment air duct adopts intercooling control mode, while the simulated battery temperature control box adopts direct cooling control mode. The refrigeration unit and heater in the temperature control system of the simulated underhood environment air duct and the simulated HVAC environment air duct control the temperature of the constant temperature water tank. The cooling water in the constant temperature water tank is connected to the inner core of the temperature and humidity control section of the air duct through pipelines, and the temperature of the simulated underhood environment

Corresponding Author: Sun Weiyi, Lecturer, Ph.D., E-mail: swy_18@jlu.edu.cn.

air duct and the inner core of the temperature and humidity control section of the simulated HVAC environment air duct are controlled through the opening of the electromagnetic valve body. The coupling effect of the power fan and the bypass fan is to supply air to the temperature control section core and the test section, In order to achieve temperature control in the testing section, simulate the underhood environment air duct and simulate the HVAC environment air duct. Dehumidification and humidification devices are installed behind the core of the temperature control section to achieve humidity control. The simulated battery temperature control box control system is equipped with a cooling unit and heater, and the internal temperature of the simulated battery temperature control box is controlled through a mixture of cold and warm air.

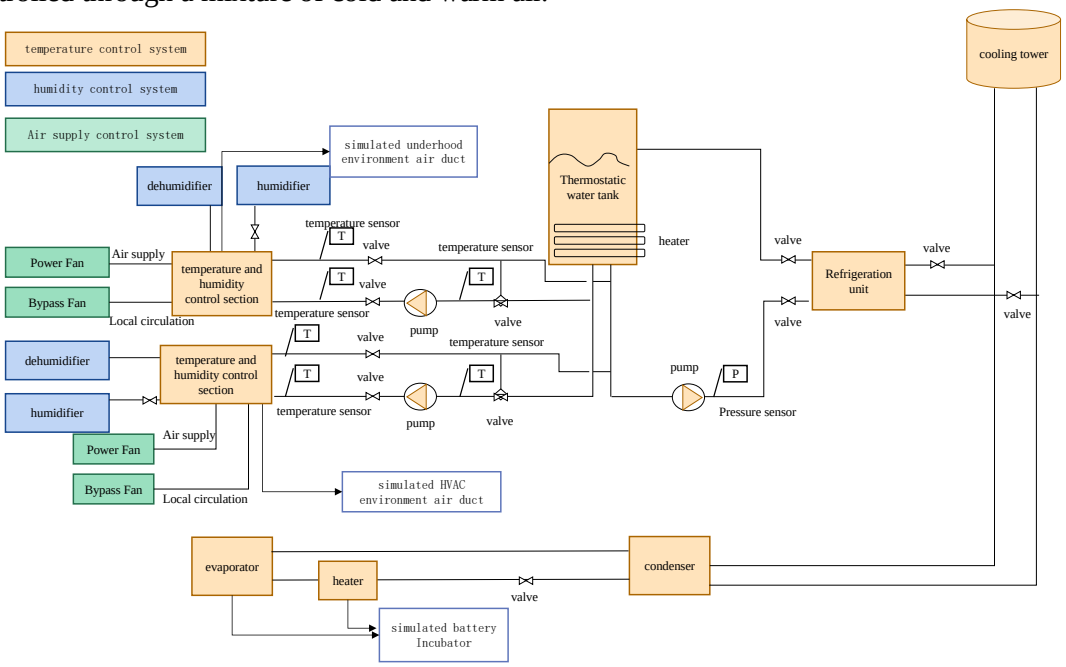

Fig. 3 System Operation Principle Diagram

3.2 Design of Air duct Structure for Simulating underhood Environment

The simulated underhood environment air duct provides constant temperature, humidity, and precise air supply for the internal components of the underhood, such as the electric drive system and front-end cooling module, consistent with the test conditions. To restore the flow field inside the actual vehicle underhood, the inlet and outlet positions of the test section, the width and axial length of the test section, and the layout and installation of the tested parts all refer to the design of the actual vehicle underhood. The air inlet of the actual engine compartment is located at the front of the radiator and condenser, and the air outlet is located on both sides below the rear of the engine compartment. Therefore, the air inlet of the test section is also designed at the front end, and the return air outlet is designed on both sides below the rear end. Considering the need for temperature and humidity control in the air duct, in order to reduce system operation energy consumption, the simulated underhood environment air duct is designed as a closed double circulation structure. As shown in Figure 4, the simulated underhood environment air duct is equipped with a power section, rectification section, testing section, side pipe section, convergence section, and temperature and humidity control section. The tested component is installed in the testing section, and the array fan is installed in the testing section. The heat transfer capacity of the temperature and humidity control system is directly related to the airflow velocity passing through the system's heat exchanger. Under low wind speed conditions,

Corresponding Author: Sun Weiyi, Lecturer, Ph.D., E-mail: swy_18@jlu.edu.cn.

the lower airflow through the temperature and humidity control system results in a decrease in the system's heat transfer capacity. If the operating conditions of the tested piece are in good agreement at this time and its transient heat production increases, the temperature and humidity control system cannot take away excess heat in a short period of time, resulting in an increase in the inlet temperature of the test section and unable to provide stable temperature air supply for the tested piece. To solve this problem, this article adds a bypass section above the temperature and humidity control section of the simulated underhood environment air duct. The installation of a circulating fan in the section aims to increase the surface flow rate of the heat exchanger, ensure the heat exchange capacity of the temperature control system at various operating points, and achieve stable temperature control.

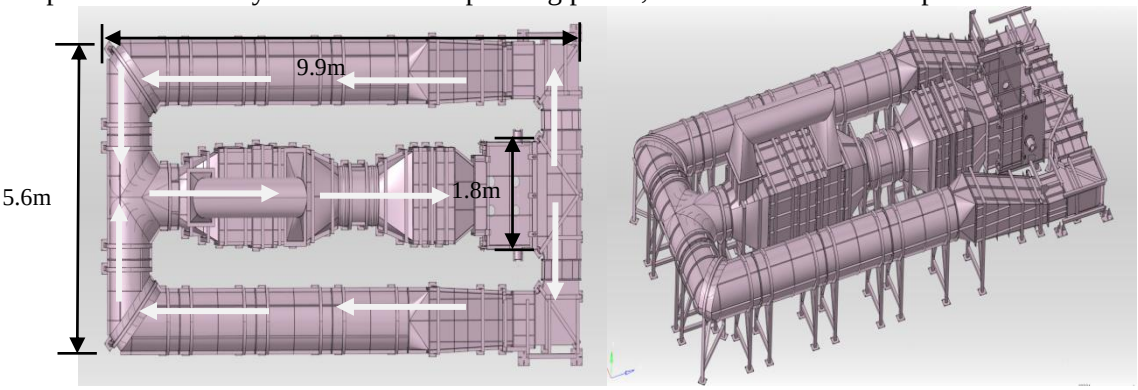

(a) Top view **(b) Oblique Side view**

Fig. 4 Top and Oblique Side view of simulated underhood environment air duct structure

The air supply range in the platform design requirements is 500m ³/ h~14000m ³/ h. The maximum wind speed change rate is 3m/s, corresponding to a flow rate change rate of 1080m ³/ h.Increasing the rotational inertia of the fan will reduce its sensitivity[14~15],According to theoretical formulas,as the Eq. 19.

$$J = (m * r^2) / 2 \tag{19}$$

J is Moment of inertia, kg / m^2 ; m is mass , kg ; r is distance from motor axis to external assembly, m .

A single large fan motor mass is 40kg, a fan blade mass of 20kg, a motor rotation radius of 0.02m, and a fan shaft radius of 0.5m. Therefore,acorresponding to the formula 20 the inertia of A single large fan motor is 2.5kg ㎡

$$T = J * \Delta\omega / \Delta t \tag{20}$$

$\Delta\omega$ is Rotation angle, Δt is time, s .determine the speed change as 100 r / s based on the change in air volume,acorresponding to the Eq. 20,the torque is 1575.024Nm. In addition, it also needs to overcome aerodynamic resistance and mechanical friction, and the total torque provided by the motor is relatively large.To reduce the rotational inertia of the fan and reduce the working load of the motor under rapidly changing wind speed conditions, it is considered to discretize a fan into several small fans. Meanwhile, considering the uniformity of the system's air supply flow rate, the number of fans should be 4, 9, 16, Considering the cost of the fan and the layout size of the air duct, a comparative study was conducted on 4 fan and 9 fan schemes. After calculation, in order to achieve rapid changes in wind speed, the torque required for each of the four fan schemes is 14.2Nm, while the torque required for each of the nine fan schemes is only 1.73Nm. Both options require a significant reduction in the torque required for the fan, which is acceptable. But by comparing the flow field distribution at the entrance of the test section between the two schemes through simulation methods, taking into

Corresponding Author: Sun Weiyi, Lecturer, Ph.D., E-mail: swy_18@jlu.edu.cn.

account both.After theoretical calculation, using traditional enonmental cabin axial flow fans, the uniformity coefficient of 9 fans became 0.9420, and the uniformity coefficient of 4 fans became 0.4298. Therefore, 9 fan schemes were ultimately selected,the array fan model is shown in Figure5.

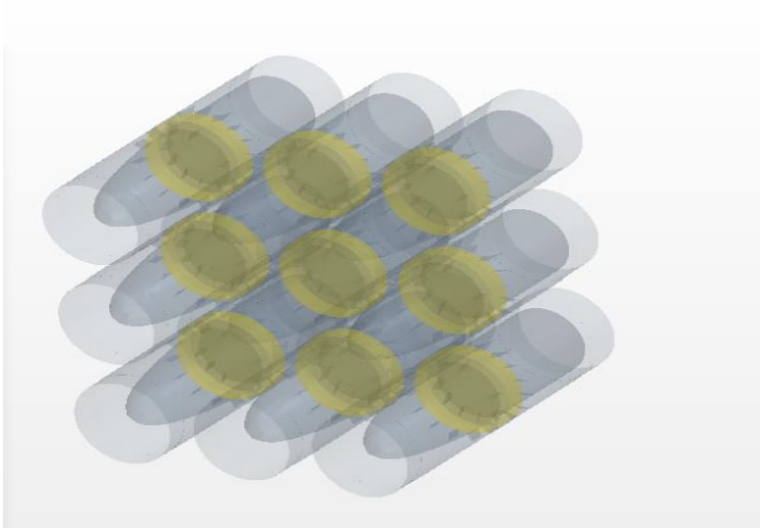

Fig. 5 Schematic diagram of array fan

3.3 Structural Design of Air Ducts in Simulated HVAC Environments

The simulated HVAC environment air duct is a closed single cycle structure, which provides target temperature, humidity, and flow intake for the evaporator or heating core in the air conditioning system. As shown in Figure 6, the simulated HVAC environment air duct includes a temperature and humidity control section, a power section, a rectification section, and a testing section. The tested core is installed in the testing section, and the array fan is installed in the power section. The airflow enters the power section after temperature and humidity control treatment through the temperature and humidity control section. It is blown downstream through the array fan and rectified through the rectification section to ensure uniform and consistent airflow towards the test section. After passing through the testing section, the airflow circulates to the temperature and humidity control section, and so on, continuously providing the required air supply for the tested object.Similar to the simulated underhood environment air duct, in order to ensure the heat transfer capacity of the temperature and humidity control system at various operating points, a bypass section was also designed for the simulated HVAC environment air duct, and a bypass fan was installed.

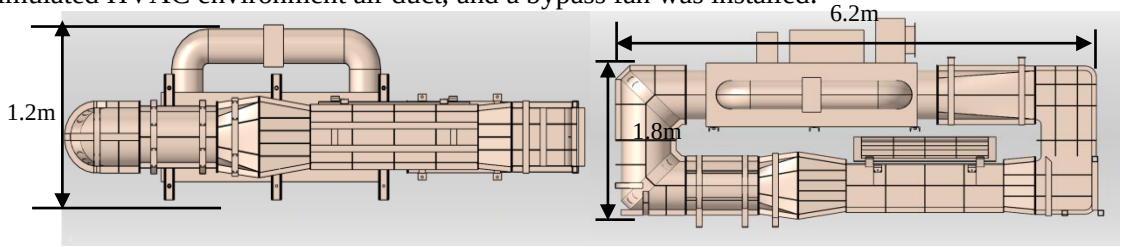

(a)Top view **(b) Oblique Side view**

Fig. 6 Top and oblique side view of simulated HVAC environment air duct structure

3.4 Structural Design of Battery Temperature Control Box

As shown in Figures 7, the battery temperature control box provides the target temperature environment for the battery system. At the same time, to simulate the thermal radiation of the battery

Corresponding Author: Sun Weiyi, Lecturer, Ph.D., E-mail: swy_18@jlu.edu.cn.

on the asphalt ground in summer, a heating plate is installed at the bottom of the box and the temperature of the heating plate is adjustable.

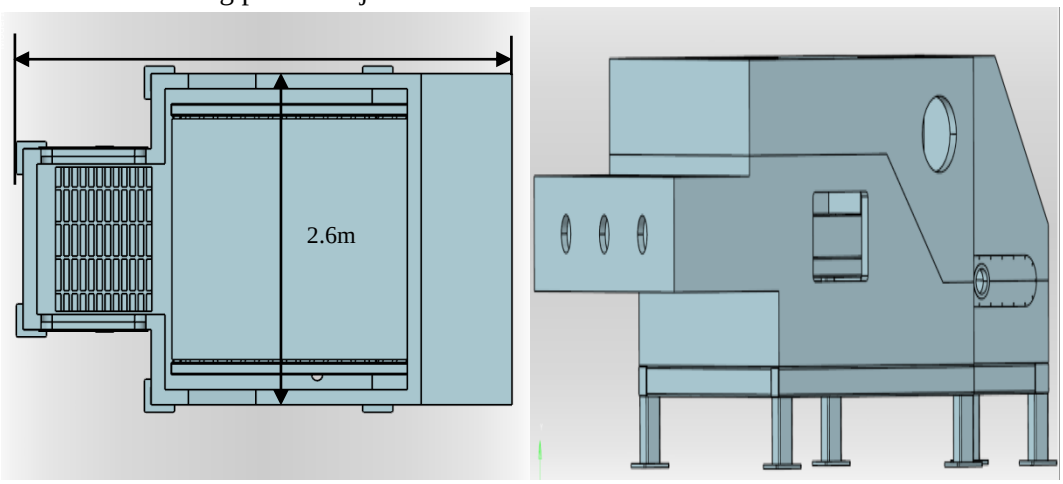

(a)Top view **(b) Oblique Side view**

Fig. 7 Top and oblique side view of battery temperature control box

The above system structure is designed based on the actual vehicle layout, which can carry real components and retain their true relative position relationships, providing a prerequisite for accurate testing. The platform relies on air supply systems, temperature control systems, and humidity control systems to provide environmental conditions that are consistent with the actual vehicle operation for the tested components. In order to restore the real environmental conditions around the components and ensure that the airflow flow, temperature, and humidity passing through each component are consistent with the real situation, it is necessary to conduct in-depth research on how the environmental air duct provides accurate temperature, humidity, and flow field environment. However, considering that temperature and humidity control technology is relatively mature, this article will not conduct in-depth research on temperature and humidity control, but will conduct in-depth research on the flow field of the integrated testing system flow field testing section. Based on the analysis of the demand environment for internal components in the cabin, the simulation of HVAC environmental air ducts and the simulation of HVAC environmental air ducts are different from environmental wind tunnels, and flow field related indicators such as boundary layer and axial static pressure gradient are temporarily not considered. The uniformity of the inlet air in front of the tested piece directly affects the velocity distribution on the surface of the heat exchanger, thereby affecting the heat transfer performance. During the actual operation of the vehicle, the intake air into the engine compartment is uniform. Therefore, in order to restore the flow field distribution on the surface of the heat exchanger, the platform needs to provide uniform intake air for the tested object. But as mentioned in Chapter 3.2, to ensure the heat exchange capacity of the heat exchanger, a bypass fan has been added to the system. The coupling between the bypass fan and the active power fan during operation directly affects the uniformity of the inlet air of the test section, and the uniformity of the inlet air in the system is the research focus. The simulated cabin environment air duct is a closed double circulation structure, with numerous internal tested components and a complex overall structure. The flow field in the system is complex, and the side ventilation fan has high power and operating speed, which greatly affects the uniformity of the test section inlet. Therefore, this article

Corresponding Author: Sun Weiyi, Lecturer, Ph.D., E-mail: swy_18@jlu.edu.cn.

takes the simulated cabin environment air duct as an example to conduct in-depth research on the uniformity of the flow field at the entrance of the test section.

4 Optimization and verification of flow field uniformity at the entrance of the testing section

The entrance of the simulated cabin environment air duct test section is connected to the test piece, and the uniformity of the inlet air directly affects the surface velocity distribution of the heat exchanger of the test piece. Therefore, the uniformity of the flow field at the test entrance should be a key research area. In the following text, simulation analysis and measurement methods will be used to solve the problem of the uniformity of the flow field at the entrance of the test section.

4.1 Optimization of velocity uniformity at the entrance of the testing section

4.1.1 Simulation Study on Flow Field Uniformity

(1) Model building

In order to improve the uniformity of the inlet air flow field of the test section, this paper applies CFD simulation analysis technology to calculate the flow field of the Simulate the underhood environment air duct. Simulation software selection starccm+ software.The model includes all the structures of the wind tunnel body, main fan, bypass fan, temperature and humidity control system heat exchanger, and corner guide structure. The main fan is an array fan composed of 9 small fans, installed in the power section. The specific model is shown in Figure8(a).As shown in in Figure8(b), the calculation domain of the model is the area inside the air duct, and the cut volume grid is selected. The grid size is 6mm~12mm. In order to obtain detailed and accurate flow field information, boundary layers are set up on the air duct and fan walls. Based on the Y+value, the thickness of the first boundary layer is calculated to be 0.1mm, with a total thickness of 10mm and 8 layers,the grid size is 26 million.

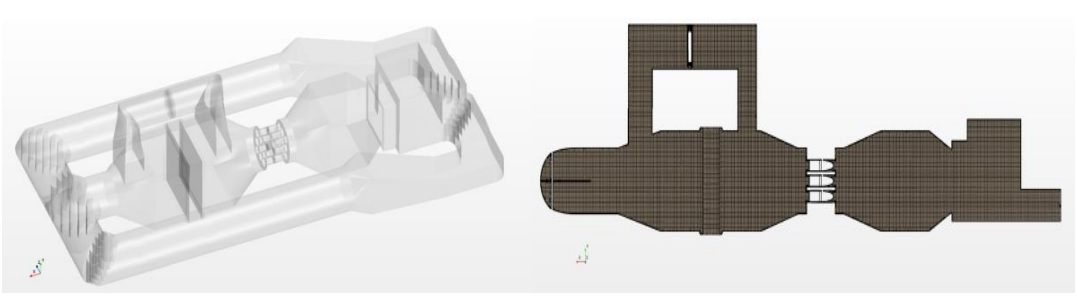

(a)geometric model **(b) Grid model**

Fig. 8 Wind tunnel model

The physical model is a three-dimensional, steady-state, gas, separated flow, K-Epsilon turbulence model[16~21], with an array fan speed of 4000r/min.

(2) Simulation results of flow field before optimization

As shown in Figure 9(a), the airflow is blown out by the array fan, and after passing through the test section, two connection sections, and corner section, it is re converged in the power section, which can achieve the function of providing continuous air supply for the tested object.However, from Figure 9(b), it can be seen that the airflow enters the stable section after being blown out by the array fan, but the airflow streamline directions are different, mixed and interfering with each other, resulting in poor flow field quality at the entrance of the testing area.

Corresponding Author: Sun Weiyi, Lecturer, Ph.D., E-mail: swy_18@jlu.edu.cn.

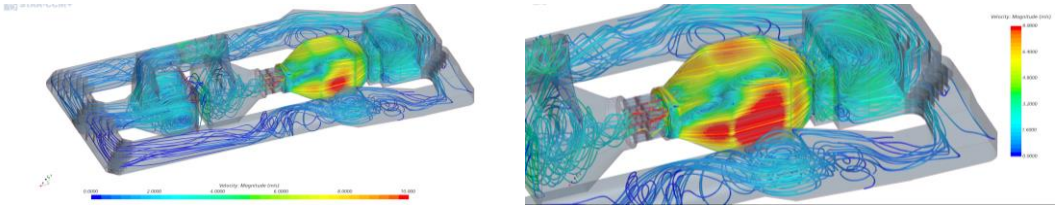

(a)whole **(b) Detail**

Fig. 9 Flow Line Diagram of Simulate the underhood environment air duct

From Figure 10, it can be seen that the airflow velocity distribution at the entrance of the test section is extremely uneven, with a uniformity coefficient of -0.0485 and a turbulence degree of 4.1228. Additionally, there is a "reflux" phenomenon in the lower right area of the section, which cannot provide uniform inflow for the tested object.

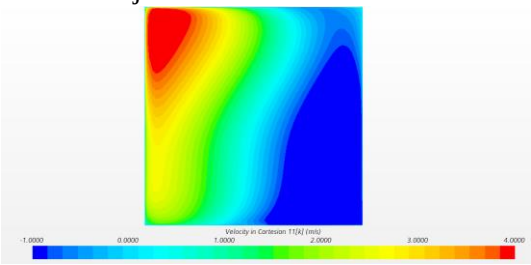

Fig. 10 Distribution of mainstream velocity direction velocity at the entrance of the testing section

4.1.2 Research on Simulation and Optimization of Flow Field Uniformity

(1) Model building

Based on the above analysis, it is necessary to sort out the airflow after the fan blows out, improve the uniformity of the inlet speed of the test section, and reduce the turbulence of the incoming flow. Adding a "honeycomb guide" structure in the air duct can suppress lateral airflow movement, cut large-scale vortices, and streamline airflow. This article selects a hexagonal honeycomb structure to comb the airflow, in order to predict the effect of adding honeycomb devices on improving the quality of the flow field. This article establishes a real honeycomb model installed in the Simulate the underhood environment air duct.

The structural size of a honeycomb directly affects the uniformity of velocity and turbulence. In order to design the optimal honeycomb structure, it is necessary to study the relationship between the width and length of the honeycomb cell, uniformity, and turbulence separately. This article uses the CFD method to simulate the flow field of honeycomb devices with different structural sizes. Due to the large number of honeycomb cells, the simulation calculation requires a lot of time and computational resources. To improve simulation efficiency, this article simplifies the simulation model and only models the rectifier region where the honeycomb is located, as shown in Figure 11.

Corresponding Author: Sun Weiyi, Lecturer, Ph.D., E-mail: swy_18@jlu.edu.cn.

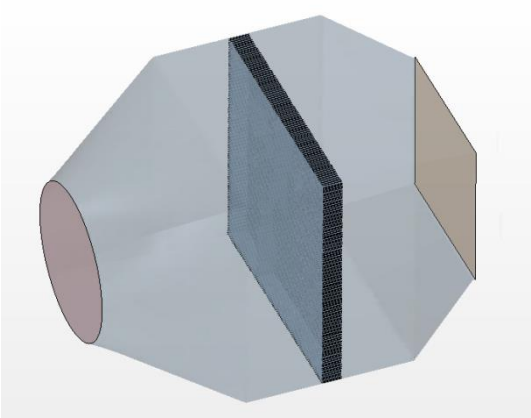

Fig. 11 Simplified Model of Honeycomb

(2) Optimization Plan Design

As shown in Figure 12, the core cell widths were calculated to be 10mm, 15mm, 20mm, and 25mm, with a honeycomb cell wall thickness of 1.5mm and a length of 100mm. The simulated grid size ranges from 67 million to 83 million.the core cell lengths are calculated to be 100mm, 150mm, 200mm, and 250mm respectively. The honeycomb cell has a wall thickness of 1.5mm, a core cell width of 10mm, and a simulated grid size of 83 million to 160 million.

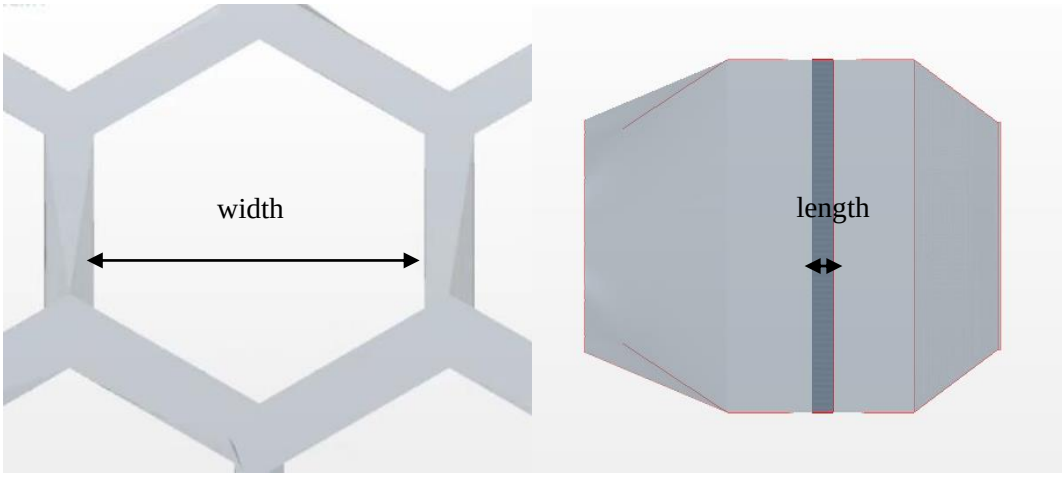

(a)width **(b) length**

Fig. 12 Schematic diagram of core cell

(3) Simulation optimization analysis

The velocity uniformity coefficient and turbulence intensity at the outlet position were obtained through simulation calculation under different core cell widths. From Figures 13(a) and (b), it can be seen that as the width of the core cell decreases, the uniformity of velocity increases, the turbulence level decreases, and the quality of the flow field improves. However, if the width of the core cell is too small, it will increase costs, increase the pressure loss of the air duct, and increase operating energy consumption. Taking into account the improvement of flow field quality, production process, and manufacturing costs, this article selects a core cell width of 10mm.

Corresponding Author: Sun Weiyi, Lecturer, Ph.D., E-mail: swy_18@jlu.edu.cn.

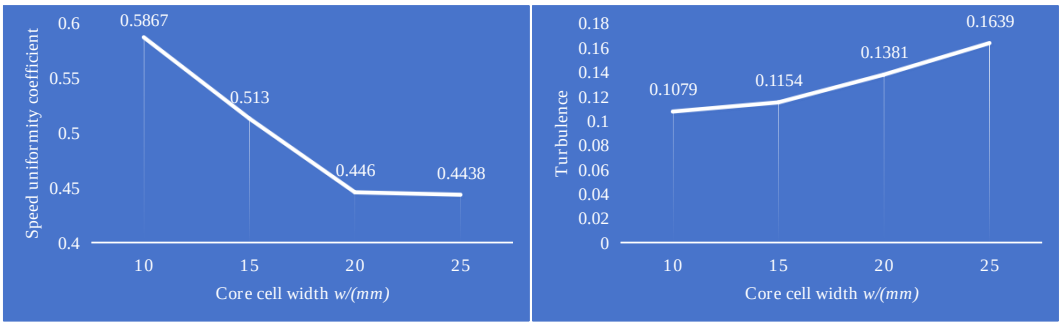

(a)Velocity Uniformity Coefficient **(b) Turbulence**

Fig. 13 Trend Chart of Variation in Velocity Uniformity Coefficient and Turbulence of Core Cells with Different Widths

From Figures 14(a) and (b), it can be seen that as the length of the core cell increases, the uniformity of velocity increases, the turbulence level decreases, and the quality of the flow field improves. But when the length increases to 150mm, the rate of turbulence decrease and the rate of velocity uniformity increase both decrease. The total length of the rectification section of the Simulate underhood environment air duct is 800mm. Considering that this section needs to be equipped with honeycomb and damping mesh structures, and a certain space area should be reserved for buffering the airflow. Therefore, this article selects a core cell length of 150mm.

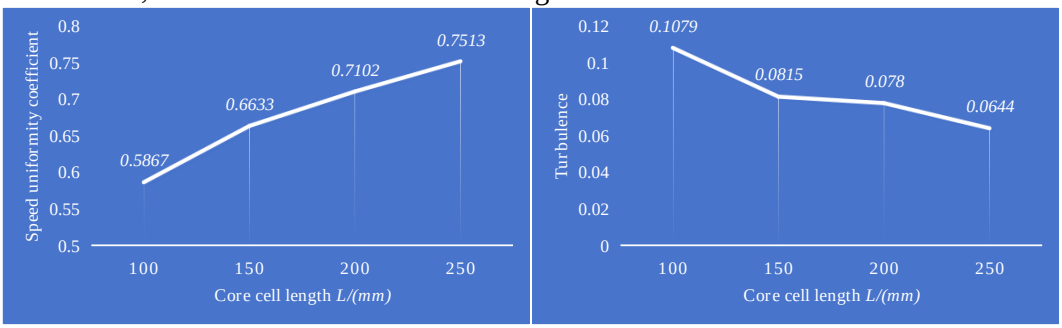

(a)Velocity Uniformity Coefficient **(b) Turbulence**

Fig. 14 Trend Chart of Variation in Velocity Uniformity Coefficient and Turbulence of Core Cells with Different lengths

A honeycomb cell with a width of 10mm and a length of 150mm was installed in the Simulate underhood environment air duct for simulation calculation. The simulation results are shown in Figure 22. Compared to Figure 15, it can be seen that after adding a honeycomb filter, the airflow is "sorted" more smoothly, with higher consistency in flow direction, and there is no "reflux" phenomenon at the entrance section of the test section. Its uniformity coefficient has been changed to 0.9420, and the turbulence degree has been changed to 0.0247. On the one hand, it can ensure uniform flow for the tested object, and on the other hand, it can provide a high-quality flow field foundation for accurate air supply.

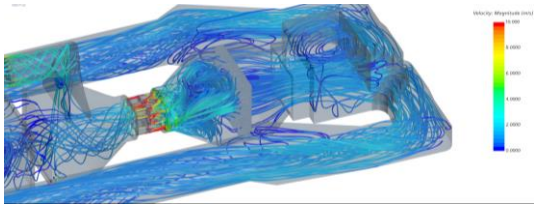

Corresponding Author: Sun Weiyi, Lecturer, Ph.D., E-mail: swy_18@jlu.edu.cn.

Fig. 15 Flow Line Diagram of Stable Section after Adding Honeycomb in Simulate the underhood environment air duct

4.2 Experimental verification of uniformity of flow field at the entrance of the testing section

After designing the platform structure and optimizing the flow field simulation, the testing platform was built and debugged. The entity of the testing platform is shown in Figure 16.

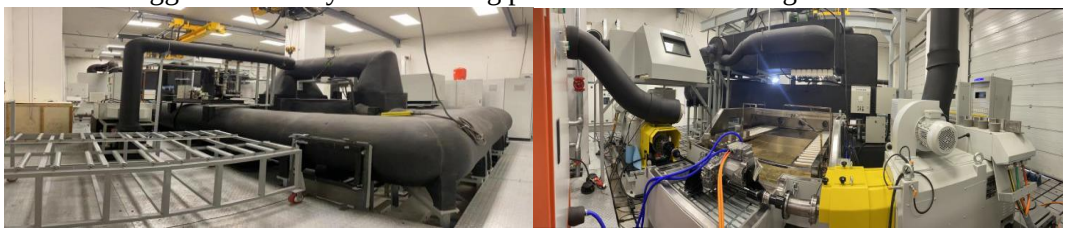

(a)Front view **(b) Side view**

Fig. 16 Front and side view Real Time of Test Platform

Before the test, a necking guide fixture is made based on the position and opening size of the tested vehicle model's grille. The necking size is 0.25m * 0.8m, and the necking guide fixture is shown in Figure 17.

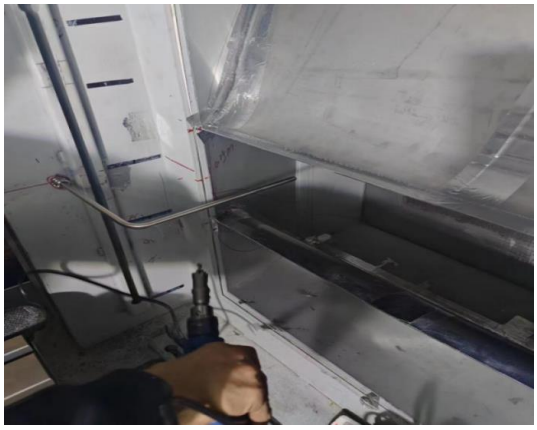

Fig. 17 Testing Shrinkage Tooling

To investigate the uniformity of the flow field before entering the grid of the tested object, this article arranges 7 flow measurement points at the outlet of the diversion necking, as shown in Figure 18. Measurement point 3 is the center position of the necking, and measurement points 1, 2, and 6 are symmetrical with measurement points 5, 4, and 7, respectively. By testing the flow rate at different measurement points under different main fan speeds, the uniformity of the flow field at the necking section of the test section was obtained.

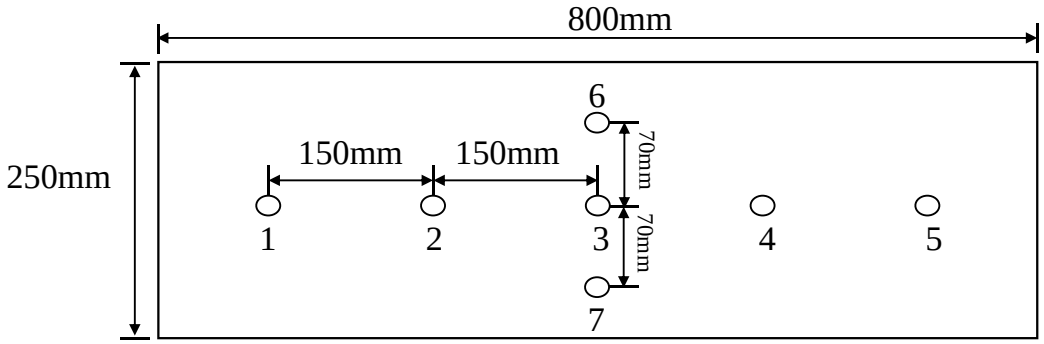

Fig. 18 Schematic diagram of the measurement points for necking speed in the test section

Corresponding Author: Sun Weiyi, Lecturer, Ph.D., E-mail: swy_18@jlu.edu.cn.

Tab. 1 Test section uniformity measurement results

Fan speed （r/min）	Flow rate at different measuring points（m3/h）							Uniformity of different measurement point positions(%)						
	1	2	3	4	5	6	7	1	2	3	4	5	6	7
500	1250.61	1239.41	1257.06	1261.68	1268.27	1250.55	1260.53	-0.39	-1.28	0.13	0.5	1.02	-0.39	0.41
1000	2889.61	2803.56	2802.11	2812.15	2841.50	2767.37	2865.46	2.25	-0.79	-0.84	-0.49	0.55	-2.07	1.40
1500	4540.44	4374.85	4428.51	4397.57	4454.27	4299.71	4454.83	2.69	-1.05	0.16	-0.54	0.74	-2.75	0.75
2000	6148.41	5926.34	5970.16	5980.58	6056.74	5816.48	6047.28	2.61	-1.10	-0.37	-0.20	1.08	-2.93	0.92
2150	6398.68	6380.57	6459.77	6458.38	6525.43	6275.67	6364.80	-0.16	-0.44	0.79	0.77	1.82	-2.08	-0.69

The test results are shown in Table 1. This article tested the necking flow rate of the main fan at the operating points of 500r/min, 1000r/min, 1500r/min, 2000r/min, and 2150r/min, and obtained the flow deviation relative to the average value at different positions. The test results show that the flow deviation at points 1-7 is less than ± 3%, with good uniformity and meeting the testing requirements.

5 Research on the Consistency of Surface Flow Field Distribution of Tested Parts

The distribution of airflow entering the engine compartment during actual operation of the vehicle is uniform, and after passing through various components in the engine compartment, the distribution on the surface of the heat exchanger is no longer uniform, which directly affects the heat transfer performance. To reflect the true heat transfer performance of the components, the platform should not only provide uniform air supply for the tested parts, but also ensure that the velocity distribution of key components on the surface of the test platform should be consistent with the velocity distribution on the actual surface of the engine room. Therefore, the following will conduct flow field simulation analysis on the tested key components installed on the testing platform and the actual vehicle cabin environment to verify the consistency of flow field distribution.

5.1 Simulation Model

5.1.1 Components mounted on the Simulate underhood environment air duct model

Through the optimization of the flow field in the previous section, it can be seen that after adding a "honeycomb" steady flow structure, the airflow velocity distribution is uniform and the flow direction is consistent. To improve simulation efficiency, the fan structure was removed from the wind tunnel underhood flow field simulation model and uniform velocity was used as the input condition for the inlet. The boundary condition is set to the mass flow inlet without specifying the pressure outlet. The inlet flow rate is set at 1.72kg/s based on the actual engine room intake air volume. Install a real model of the interior components of the vehicle underhood in the wind tunnel test section, and its geometric model is shown in Figure 19 (a).

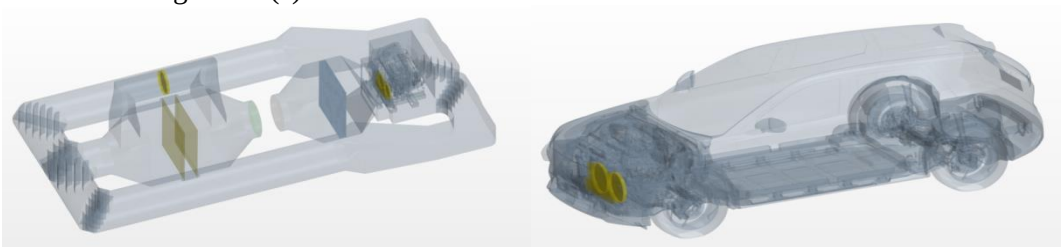

(a)Simulate underhood environment air duct (b)Real vehicle

Fig. 19 geometric model Geometric Model of Components Mounted in the Simulate underhood environment air duct

Corresponding Author: Sun Weiyi, Lecturer, Ph.D., E-mail: swy_18@jlu.edu.cn.

5.1.2 Components mounted in the actual vehicle underhood model

Select a certain actual vehicle and establish a full detail model of the entire vehicle, which includes the exterior design of the vehicle body, detailed components in the engine compartment, floor and chassis components, etc., as shown in Figure19 (b).

5.2 Comparison and Analysis of Simulation Results

5.2.1 Analysis of the calculation results of the inlet air volume of the heat exchanger

The intake air volume of the heat exchanger directly affects the heat transfer performance of the heat management system. Through simulation calculations, the intake air volume of the heat exchanger in the Simulate underhood environment air duct and the actual vehicle underhood are obtained.

Tab. 2 Comparison of Heat Exchanger Inlet Air Volume

	Simulate underhood environment air duct	vehicle	error（%）
Radiator inlet air volume（kg/s）	0.5011	0.5013	0.039
Inlet air volume of condenser（kg/s）	0.8743	0.8928	2.116

As shown in Table 2, the intake air volume of the radiator and condenser in the Simulate underhood environment air duct environment is 0.5011kg/s and 0.8743kg/s respectively. The intake air volume of the radiator and condenser in the actual engine compartment environment is 0.5013kg/s and 0.8928kg/s respectively. The error in the intake air volume of the radiator is 0.039%, and the error in the intake air volume of the condenser is 2.116%.

5.2.2 Analysis of calculation results of flow field around key components

As mentioned earlier, the intake air volume of the heat exchanger directly affects the heat transfer performance of the thermal management system and is a key component in the underhood. In addition, the electric drive assembly, as the main heat source in the underhood, is also a key focus of the thermal management system. Therefore, this article focuses on comparing the surface velocity distribution of the radiator and condenser, as well as the flow field distribution around the electric drive assembly. As shown in Figures 20, due to the shape of the grille in front of the radiator, the flow velocity in the middle area of the radiator is extremely low, and the flow velocity on the left and right sides is high, with a velocity distribution between 8m/s and 10m/s. The radiator is located in the Simulate underhood environment air duct, and its surface velocity distribution is highly consistent with the surface velocity distribution of the radiator in the actual engine compartment environment.

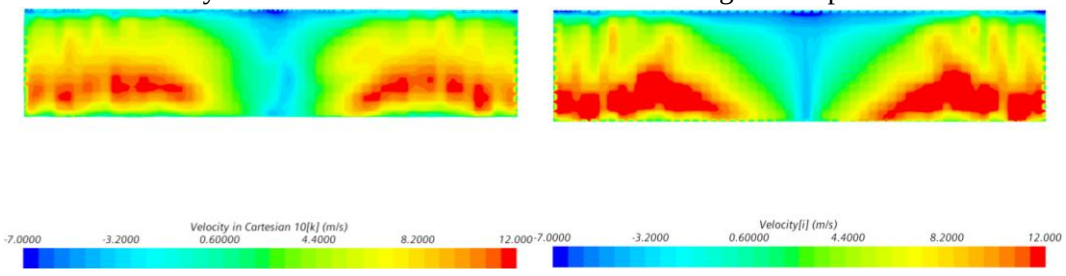

(a)air duct environment (b) real vehic environmentl

Fig. 20 velocity distribution of Radiator

As shown in Figures 21, the condenser is located in both the Simulate underhood environment air ductenvironment and the actual engine compartment environment, with a speed range of between 6m/s and 9m/s, and its surface velocity distribution trend remains basically consistent.

Corresponding Author: Sun Weiyi, Lecturer, Ph.D., E-mail: swy_18@jlu.edu.cn.

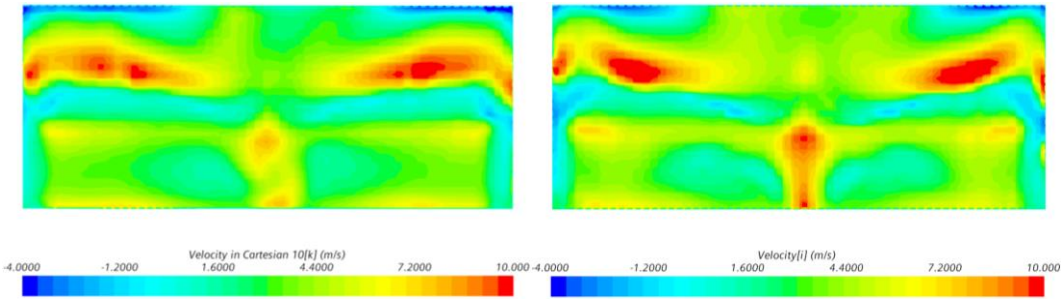

(a) air duct environment **(b) real vehic environmentl**

Fig. 21 velocity distribution of condensert

As shown in Figures22, the electric drive assembly is installed in the Simulate underhood environment air duct and the actual vehicle underhood, with a velocity distribution range of 4m/s to 8m/s, and the velocity distribution trend remains consistent in the Simulate underhood environment air duct and the actual vehicle underhood environment.

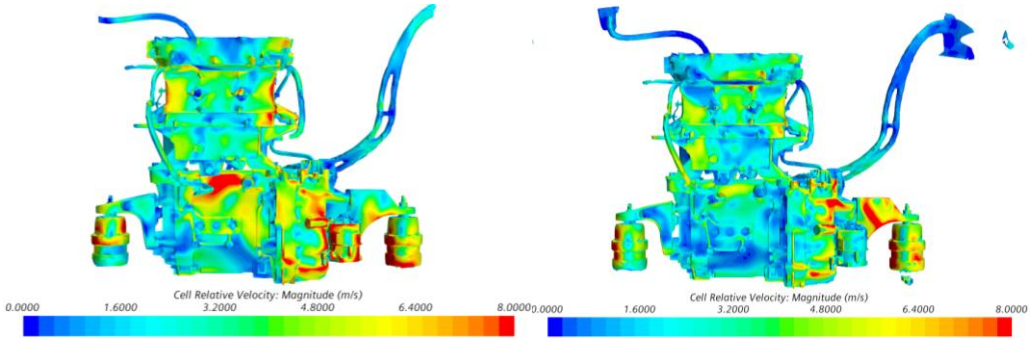

(a) air duct environment **(b) real vehic environmentl**

Fig. 22 Velocity distribution of electric drive assembly

Based on the above analysis, it can be concluded that the flow field environment provided by the Simulate underhood environment air duct is highly consistent with the environment inside the actual vehicle underhood, which can ensure that the system's heat generation and dissipation performance is close to the real situation and meet the requirements of thermal management system integration testing.

6 Summary

(1) This paper, based on the working principles of key components in the thermal management system, identifies the environmental conditions that the testing system needs to provide for the test subject and proposes a novel integrated thermal management testing system configuration. To enhance the uniformity of the velocity distribution at the entrance of the test section, simulations were conducted to optimize different structural dimensions of the honeycomb. Ultimately, the width of the honeycomb was determined to be 10mm, with a length of 150mm.

(2) Comparative analysis using simulation methods was performed to assess the degree of alignment between the flow field within the components in the test section and the flow field inside a real vehicle cabin. The results show a high degree of alignment between the flow field of the test subject within the system and the flow field inside a real vehicle cabin. The overall intake airflow error for the radiator was 0.039%, and the condenser intake airflow error was 2.116%. Furthermore, the flow field distribution around the radiator, condenser, and electric drive assembly exhibited good consistency. Additionally, this system can accommodate actual components while retaining their real relative

Corresponding Author: Sun Weiyi, Lecturer, Ph.D., E-mail: swy_18@jlu.edu.cn.

positional relationships, meeting the requirements of integrated testing for thermal management systems.

(3) This testing system is primarily used to simulate the real operating conditions of a vehicle at the system level, enabling the execution of real transient condition tests. During transient vehicle operation, the cabin's intake airflow fluctuates continuously. Currently, this paper has not delved into an in-depth study of how the test stand can provide consistent and precise transient airflow rates that match the operation of a real vehicle. This will be a focus of future research.

Acknowledgment (Word Style TS Strong)

This research is funded by Youth Foundation of National Natural Science Foundation of China (No.52102458) and Major Science and Technology Projects in Jilin Province and Changchun City (Grant No. 20210301023GX；20220301010GX).

References

[1] Jia M X., *et al*.,Progress and perspectives of integrated thermal management systems in PEM fuel cell vehicles:A review, Renewable and Sustainable Energy Reviews, 2022, 3, pp. 155

[2] Lv Feng., The investigation on match and design of commercial vehicle cooling module, Zhe Jiang University,2011,pp. 45-56.

[3] Zhao Y B., Study on Thermodynamic Model of New Energy Vehicle Thermal Management System Testbed, Science&Technology informaiton,2021,19,33,pp. 58-61

[4] Wang W M., *et al*.,Research on Development Technologies of Thermal Management System with Heat Pump for Battery Electric Vehicles. Chinese Journal of Automotive Engineering,2021,11,6,pp. 434-441

[5] Xue S., Development and Research of Test Platform for Electric Vehicle Thermal Systems Cooperative Management,Zhe Jiang University,2012,pp. 37-44

[6] MA J., *et al*., Experimental study on the performance of vehicle integrated thermal management system for pure electric vehicles,Energy Conversion and Management,2022,1,pp. 2

[7] Li W B., *et al*.,Coupled thermal electrochemical model of 3D lithiumion battery,Chinese Journal of Power Sources, 2016, 40,7,pp. 1362-1366

[8] FU Y., Research and Optimization on Thermal Management of Engine Compartment of an Agricultural Machinery, Ji Lin University,2021,pp. 34-42

[9] Geng Y L., Research on Heat Dissipation of Commercial Vehicle Engine Compartment Based on 1D/3D Co-simulation, Ji Lin University,2021,pp. 59-61

[10] Y L., *et al*.,Establishment and Analysis of A Simulation Model for An Electric Vehicle’s Thermal Load,The Journal of New Industrialization, 2019, 9（5）,pp. 70

[11] Liang S C., Study on Effect of Temperatureon Resistance of Li-ion Battery.Guangzhou Chemical Industry,2018,46 ,15,pp. 66-67

[12] Liu X T., *et al*.,State-of-Power Estimation for Li-ion Battery Considering the Effect ofTemperature,Transactions of China Electro Technical Society,2016,31(13),pp. 156.

Corresponding Author: Sun Weiyi, Lecturer, Ph.D., E-mail: swy_18@jlu.edu.cn.

[13] Tete P R., *et al*.,Developments in battery thermal management systems for electric vehicles:A technical review, Journal of Energy Storage, 2021, 3,pp. 35
[14] Cao S Y., *et al*.,Reproduction of wind velocity history in a multiple fan wind tunnel. Wind Eng. Ind.Aerodyn,2002,90 (12-15),pp. 1719-1729
[15] Shao P L., *et al*.,Active Simulation of Transient Wind Field in a Multiple-Fan Wind Tunnel via Deep Reinforcement Learning,Wind Eng. Ind.Aerodyn,2021,147,pp. 9
[16] Hu Xingjun., *et al*.,Low wind drag numerical research on fenders and wheels of car model,Applied Mechanics and Materials,2013,(397-400),pp. 599-602
[17] Zhang Y., *et al*.,Transient simulation research on automobile aerodynamic lift based on LBM method,Mechanics of fluids and gases,2017,23(6)
[18] Mason M S., *et al*.,Numerical simulation of downburst winds,Wind Eng,Ind. Aerodyn,2009,34(12),pp. 523–539
[19] Teunissen H W., Simulation of the planetary boundary layer in a multiple-jet wind tunnel,Atmos. Environ,1975,9 (2),pp. 145-174.
[20] Bienkiewicz B., *et al*., Active modeling of large-scale turbulence,Wind Eng,Ind. Aerodyn,1983,13 (1-3),pp. 465-475
[21] KobayashiI H., *et al*.,Active generation of wind gust in a two dimensional wind tunnel. Wind Eng. Ind. Aerodyn,1992,42 (1-3),pp. 959-970

Submitted: 26.09.2023.
Revised: 30.09.2023.
Accepted: 08.11.2023.

Corresponding Author: Sun Weiyi, Lecturer, Ph.D., E-mail: swy_18@jlu.edu.cn.